J|A|C|S COMMUNICATIONS

Published on Web 10/28/2010

Intramolecular Hydroamination/Cyclization of Aminoalkenes Catalyzed by $Ln[N(SiMe_3)_2]_3$ Grafted onto Periodic Mesoporous Silicas

Erwan Le Roux,[†] Yucang Liang,[†,‡] Michael P. Storz,[†] and Reiner Anwander*[,†,‡]

Department of Chemistry, Universitetet i Bergen, Allégaten 41, N-5007, Bergen, Norway, and Institut für Anorganische Chemie, Universität Tübingen, Auf der Morgenstelle 18, D-72076, Tübingen, Germany

Received September 6, 2010; E-mail: reiner.anwander@uni-tuebingen.de

Abstract: Homoleptic rare-earth metal silylamide complexes $Ln[N(SiMe_3)_2]_3$ (Ln = Y, La, Nd) were grafted onto a series of partially dehydroxylated periodic mesoporous silica (PMS) supports, SBA-15_{-500} (d_p = 7.9 nm), SBA-$15LP_{-500}$ (d_p = 16.6 nm), and MCM-41_{-500} (d_p = 4.1 nm). The hybrid materials $Ln[N(SiMe_3)_2]_3$@PMS efficiently catalyze the intramolecular hydroamination/cyclization reaction of 2,2-dimethyl-4-penten-1-amine. Under the prevailing slurry conditions the metal size (Y > La > Nd), the pore size, and the particle morphology affect the catalytic performance. Material $Y[N(SiMe_3)_2]_3$@SBA-$15LP_{-500}$ displayed the highest activity (TOF = up to 420 h^{-1} at 60 °C), with the extralarge pores minimizing restrictive product inhibition and substrate diffusion effects. The catalytic activity of $Y[N(SiMe_3)_2]_3$@SBA-$15LP_{-500}$ is found to be much higher than that of the molecular counterpart (TOF = up to 54 h^{-1}), and its recyclability is demonstrated.

The hydroamination of unsaturated carbon−carbon bonds is a prominent, highly atom-efficient reaction for the synthesis of nitrogen-containing compounds.[1] Particularly, intramolecular hydroamination/cyclization (IHC) displays an efficient route for accessing multifunctional N-heterocycles of relevance for natural product synthesis and hence pharmaceuticals.[2] Since the seminal discovery of organolanthanide(metallocene)-catalyzed IHC by Marks and co-workers,[3] this and related olefinic transformations emerged as a most prolific branch of rare-earth metal-based homogeneous catalysis.[4] Both metallocene and nonmetallocene complexes were found to provide high catalytic activities and stereoselectivities.[5−7] Setting out from aminoalkenes[3−7] the scope of Ln^{3+}-promoted IHC transformations was quickly extended to various unsaturated molecules including aminoalkynes,[5b,8] aminoallenes,[9] conjugated aminodienes[10] and aminodialkenes, aminodialkynes, and aminoalkenalkynes.[11] Easy and complete product/catalyst separation is crucial for the production of highly pure biologically active compounds and best achieved via heterogeneous catalysis. So far, only the homogeneous IHC catalysts $(C_5Me_5)_2Ln[CH(SiMe_3)_2]$ (Ln = La, Sm) and $[Me_2Si\{(C_5Me_4)(N\mathit{t}Bu)\}]Sm[N(SiMe_3)_2]$ were ingeniously immobilized in situ on various amino-functionalized polystyrene resins.[12] A flexible catalyst↔support binding allowed the release and recapturing of the catalyst after IHC completion. Some of these polymer-supported catalysts displayed activities comparable to those of their homogeneous counterparts (e.g., TOF ≈ 22.5 versus 30 h^{-1}), showing only minor to moderate loss of activity upon recycling.[12] This contribution represents the first heterogenization of rare-earth metal catalysts on inorganic supports for the IHC reaction. Aiming at well-defined heterogeneous catalysts,[13] we found that materials $Ln[N(SiMe_3)_2]_3$@PMS (PMS = *p*eriodic *m*esoporous *s*ilica) display excellent catalytic activities for the transformation of 2,2-dimethyl-4-penten-1-amine (**1a**) into pyrrolidine (**1b**), with the pore diameter and morphology of the PMS material crucially affecting the catalytic performance.

The PMS support and active rare-earth metal component were chosen on the basis of the following criteria: (a) PMSs emerged as versatile supports offering high surface areas and an easily tunable pore size/configuration;[14,15] (b) "simple" $Ln[N(SiMe_3)_2]_3$ (**2**) were shown to serve as efficient IHC catalysts;[16] (c) the surface chemistry of **2** on silica materials is well-understood.[17] Keeping in mind the implications of both the pore size and Ln^{3+} size for the catalytic performance,[18] we initially selected SBA-15[19] as a relatively large pore PMS as well as yttrium, lanthanum, and neodymium as rare-earth metal centers. Accordingly, the solution grafting of 0.5 equiv of **2a**−**c** in hexane at ambient temperature onto SBA-15, partially dehydroxylated at 500 °C (denoted as SBA-15_{-500}), gave hybrid materials $Y[N(SiMe_3)_2]_3$@SBA-15_{-500} (**3a**), $La[N(SiMe_3)_2]_3$@SBA-15_{-500} (**3b**), and $Nd[N(SiMe_3)_2]_3$@SBA-15_{-500} (**3c**), via Ln−N bond protonolysis (Scheme S1).[17] All of the organometallic−inorganic hybrid materials were characterized by elemental analysis and DRIFT and $^1H/^{13}C$ NMR spectroscopies (Table S1, Figures S2 and S3), suggesting a mixture of $\{(\equiv SiO)Ln[N(SiMe_3)_2]_2\}$ (∼40%, monopodal) and $\{(\equiv SiO)_2Ln[N(SiMe_3)_2]\}$ (∼60%, bipodal) surface species.[17a,b,d]

Parent SBA-15_{-500} and the hybrid materials **3a**−**c** were further characterized by nitrogen physisorption (Figure S4, Table S1). Analysis of the Barret−Joyner−Halenda (BJH) pore size distribution revealed a consistent decrease of the pore diameter ($\Delta d_p \approx$ 1.2−1.4 nm) for all grafted materials (**3a**−**c**). While the filling of the mesopores was clearly indicated, the intrinsic mesoporosity was retained (type-IV isotherms).[14,18]

The catalytic activity of $Ln[N(SiMe_3)_2]_3$@SBA-15 (**3a**−**c**) for the IHC reaction was examined employing 2,2-dimethyl-4-penten-1-amine (**1a**) as a routine substrate at 50 °C in benzene-d_6 on the NMR scale and compared to that of the homogeneous yttrium counterpart **2a** (Table 1, runs 1−4, Figure 1).[20] All IHC reactions using the supported precatalysts **3a**−**c** proceeded rapidly and cleanly to the cyclized product **1b**, while the homoleptic complex **2a** showed a higher activity (TOF_i = 54 h^{-1}). Surprisingly, the heterogenized silylamido catalysts exhibited the highest activity for yttrium as the rare-earth metal center (run 2), contrary to previous results where the TOFs usually increase with the ionic radii of the Ln^{3+} center.[21]

The conversion versus time plots for the IHC catalyzed by $Ln[N(SiMe_3)_2]_3$@SBA-15_{-500} (**3a**−**c**) feature a plateau (Figure 1), characteristic for heterogeneously catalyzed reactions, where restricted diffusion of the substrate/product becomes prominent with

[†] Department of Chemistry, Universitetet i Bergen.
[‡] Institut für Anorganische Chemie, Universität Tübingen.

 10.1021/ja107963u © 2010 American Chemical Society

Table 1. Catalytic Performance of $Y[N(SiMe_3)_2]_3$@PMS in the IHC of 2,2-Dimethyl-4-penten-1-amine (**1a**)[a]

run	catalyst	*T* (°C)	Time[f] (h)	TOF[g] (h^{-1})
1	$Y[N(SiMe_3)_2]_3$ (**2a**)[b]	50	1.9	54/16
2	$Y[N(SiMe_3)_2]_3$@SBA-15 (**3a**)[b]	50	8.6	39/4
3	$La[N(SiMe_3)_2]_3$@SBA-15 (**3b**)[b]	50	11.4	36/3[h]
4	$Nd[N(SiMe_3)_2]_3$@SBA-15 (**3c**)[b]	50	14.1	26/1[i]
5	$Y[N(SiMe_3)_2]_3$@SBA-15LP (**4a**)[b]	50	0.9	74/36
6	$Y[N(SiMe_3)_2]_3$@SBA-15LP (**4a**)[c]	30	0.8	27/19
7	$Y[N(SiMe_3)_2]_3$@SBA-15LP (**4a**)[c,d]	30	3.2	17/5
8	$Y[N(SiMe_3)_2]_3$@SBA-15LP (**4a**)[c,e]	30	7.6	6/1[j]
9	$Y[N(SiMe_3)_2]_3$@SBA-15LP (**4a**)[c]	50	0.3	95/48
10	$Y[N(SiMe_3)_2]_3$@SBA-15LP (**4a**)[c,d]	50	7.0	15/2
11	$Y[N(SiMe_3)_2]_3$@SBA-15LP (**4a**)[c]	60	0.2	417/105
12	$Y[N(SiMe_3)_2]_3$@SBA-15LP (**4a**)[c]	70	<0.1	−[k]/>225
13	$Y[N(SiMe_3)_2]_3$@SBA-15LP (**4a**)[c,d]	70	0.3	82/49
14	$Y[N(SiMe_3)_2]_3$@SBA-15LP (**4a**)[c,e]	70	15.6	7/1
15	$Y[N(SiMe_3)_2]_3$@MCM-41 (**5a**)[b]	50	0.3	16/10
16	$Y[N(SiMe_3)_2]_3$@SiO_2 (**6a**)[b]	50	10.0	21/4[g,l]

[a] Reaction conditions: in benzene-d_6 (0.7 mL). [b] 2.85 mol % cat. [c] 5.70 mol % cat. [d] 1st recycling. [e] 2nd recycling. [f] Time required for 90% conversion. [g] Initial TOF versus overall TOF (taken at 90% conversion, unless otherwise stated). [h] At 80% conversion. [i] At 55% conversion. [j] At 25% conversion. [k] Conversion complete after <3 min. [l] Reaction conditions: in benzene-d_6 (1.7 mL).

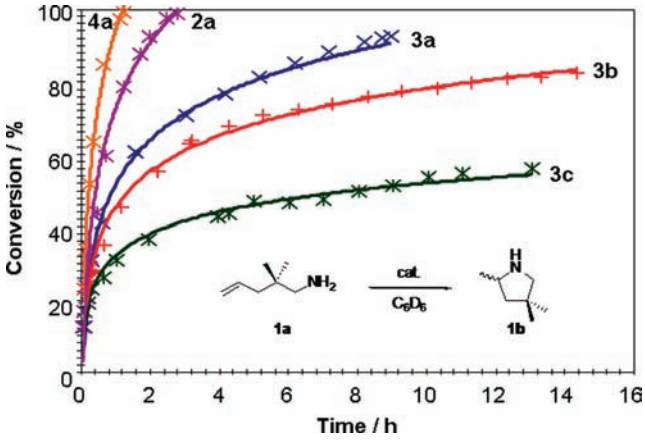

Figure 1. Conversion versus time plots for the IHC of **1a** using $Y[N(SiMe_3)_2]_3$@SBA-15LP (**4a**, orange), $Y[N(SiMe_3)_2]_3$ (**2a**, magenta), $Y(N(SiMe_3)_2)_3$@SBA-15 (**3a**, blue), $La[N(SiMe_3)_2]_3$@SBA-15 (**3b**, red), and $Nd[N(SiMe_3)_2]_3$@SBA-15 (**3c**, green) (cf., Table 1, runs 1−5). Lines are drawn only as a guide.

increasing conversion. The unsupported complex **2a** shows also a slight curve inflection after the first half-life. This has been already observed for rare-earth metal silylamide complexes, where the rate law is generally admitted to be different from zero-order in aminoalkene concentration.[3a,5,6b,7c,e] For the silica supported catalysts **3a**−**c** the curve inflections are already distinct at 20% conversion, suggesting a substantial competitive product inhibition (e.g., formation of metal secondary amine adduct species) which could be enhanced by pore confinement of the product. Moreover, formation of inactive surface species through thermal decomposition of the supported lanthanide silylamido species (formation of trisiloxy rare-earth metal [(≡SiO)$_3$Ln] and silazane [≡SiNHR] surface species) cannot be totally excluded.[22]

In order to unveil the pore confinement hypothesis, we investigated two more hexagonal channel-like PMS materials with two extreme pore sizes, MCM-41$_{-500}$ (regular small pore, $d_p = 4.1$ nm)[23] and SBA-15LP$_{-500}$ (extralarge pore, $d_p = 16.6$ nm),[24] as well as an amorphous silica, SiO_2(Aerosil300)$_{-500}$. With the same grafting conditions applied (vide supra), hybrid materials

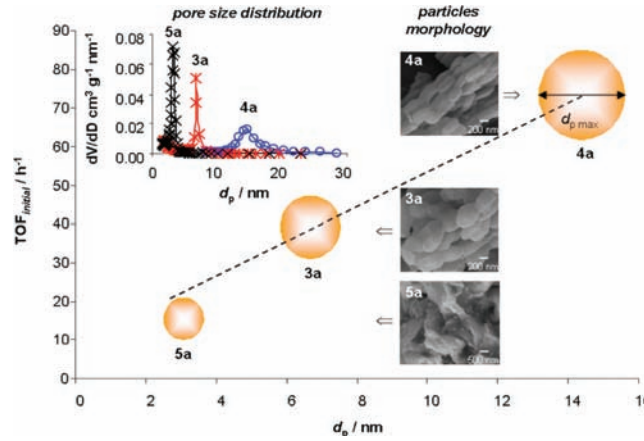

Figure 2. Initial turnover frequency TOF_i of the catalyzed IHC versus maximum pore diameter $d_{p\ max}$ (from BJH pore size distributions, adsorption branch) and particle morphology (SEM micrographs), for $Y[N(SiMe_3)_2]_3$@SBA-15 (**3a**), $Y[N(SiMe_3)_2]_3$@SBA-15LP (**4a**), and $Y[N(SiMe_3)_2]_3$@MCM-41 (**5a**) (cf. Table 1: runs 2, 5, and 15).

$Y[N(SiMe_3)_2]_3$@SBA-15LP$_{-500}$ (**4a**), $Y[N(SiMe_3)_2]_3$@MCM-41$_{-500}$ (**5a**), and $Y[N(SiMe_3)_2]_3$@$SiO_{2\text{-}500}$ (**6a**) were obtained and fully characterized (Table S1, Figures S5 and S6). The nitrogen adsorption/desorption isotherms of materials **4a** and **5a** (Table S1, Figure S7) revealed that mesoporosity was retained (type-IV isotherms) with a major change of pore size for **4a** compared to the parent SBA-15LP silica ($\Delta d_p \approx 2.2$ nm; **3a**: $\Delta d_p \approx 1.2$ nm; **5a**: $\Delta d_p \approx 1.0$ nm). Note that the pore size of **4a** is at least 2-fold and 4-fold larger than in the case of **3a** and **5a**, respectively (14.4 nm versus 6.7 and 3.1 nm).

As anticipated, hybrid material $Y[N(SiMe_3)_2]_3$@SBA-15LP$_{-500}$ (**4a**) with the extralarge pores displayed a much better catalytic performance ($TOF_i \approx 74\ h^{-1}$, up to 99% conversion after 75 min; Table 1, run 5, and Figure S10) than large-pore material $Y[N(SiMe_3)_2]_3$@SBA-15$_{-500}$ (**3a**). Further, the heterogenized catalyst **4a** exhibited a higher activity than the homogeneous counterpart **2a**. The latter phenomenon and accelerated IHC reaction rate can be ascribed to a bulkier, more electron-withdrawing silica ligand.[3a,6a,c,25] Raising the reaction temperature to 60 °C boosted the initial TOFs to 417 h^{-1} (Table 1, run 11). Even at 70 °C, degradation of the catalytically active species seems not to be distinct (Table 1, run 12). In accordance with the pore confinement hypothesis, $Y[N(SiMe_3)_2]_3$@MCM-41$_{-500}$ (**5a**) with a considerably smaller pore diameter was less active in the IHC reaction ($TOF_i \approx 16\ h^{-1}$; Table 1, run 15). Nevertheless, by plotting the pore diameter d_p against the initial TOF, a slightly better performance was expected for yttrium catalyst **5a** (Figure 2). This mismatch is attributed to not only the concurrence of various effects, including product inhibition and substrate diffusion, but also a different dispersion behavior of the MCM-41-derived material. Hybrid materials **3a** and **4a** feature a similar necklace-like particle morphology with an average size of 20 μm (long) × 2 μm (diameter), while **5a** is composed of nonregular particles with an average size of 25−35 μm, as evidenced by SEM micrographs (Figures 2, S8, and S9). As a consequence, hybrid materials **3a** and **4a** stay well dispersed in solution for hours limiting any mass transfer effect (same activities were observed with and without agitation). This is not the case for MCM-41-based **5a**, which disperses poorly, or for $Y[N(SiMe_3)_2]_3$@$SiO_{2\text{-}500}$ (**6a**), producing a sticky gel even in larger amounts of bezene-d_6 (solvent-sponge).

Detailed kinetic studies on the transformation of **1a** → **1b** using **4a** at 50 °C revealed that the reaction rate is still catalyst-dependent (first-order, Figure S11) but show a constant deviation from zero-

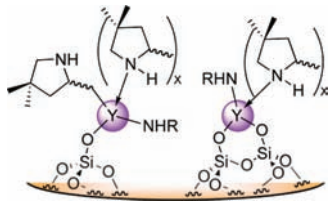

Figure 3. Proposed surface species of recycled catalyst Y[N(SiMe$_3$)$_2$]$_3$@SBA-15LP (**4a**); most likely due to product inhibition any detectable catalytic activity is lost after the third recycling step.

order linearity after the first half-life with variable substrate concentrations (Figures S12−S16), as previously reported for Ln amide catalysts.[3,7d,10b,16a] In our case, product inhibition is more pronounced due to the presence of predominantly pore-confined active sites. Analysis of the Eyring and Arrhenius plots implies highly constrained transition states ($\Delta H^{\ddagger} = 41.6(2.7)$ kJ mol^{-1} and $\Delta S^{\ddagger} = -136(8)$ J mol^{-1} K^{-1}) suggesting a similar IHC mechanism and TON-limiting olefin insertion into Ln−N bonds as previously reported, albeit the activation energy ($E_a = 46.9(2.8)$ kJ mol^{-1}) for heterogenized **4a** is lower (Figures S17/S18).[3a,26]

The supported catalyst Y[N(SiMe$_3$)$_2$]$_3$@SBA-15LP$_{-500}$ (**4a**) could be recovered and reused twice for this very transformation at different temperatures (Table 1, runs 6−10 and 12−14) albeit with a substantial loss of activity for every recycling step. Leaching of any active Y species could be excluded, since addition of a second batch of **1a**, either to the filtered supernatant or the supernatant nonvolatiles, did not produce any IHC activity. Investigations into the surface species after the second recycling step by DRIFT spectroscopy showed three weak ν_{NH} absorptions (3351, 3291, and 3077 cm^{-1}) attributable to [Y(NHR)$_x$(NHR$_2$)$_y$] moieties (Figures 3 and S19).[3a] Addition of isopropyl alcohol to this recycled catalyst gave an average of ∼1.0−1.3 equiv of **1a** and ∼4.2−5.1 equiv of **1b** per Y metal center, indicative of a pronounced product inhibition.[27]

In summary, we have shown that simple rare-earth metal silylamide complexes Ln[N(SiMe$_3$)$_2$]$_3$ display considerably higher catalytic activity in the IHC of aminoalkenes when grafted onto PMS (Y > La > Nd). Crucially restrictive product inhibition and substrate diffusion effects can be minimized by the use of an extralarge pore PMS material. Under the prevailing slurry conditions the particle morphology seems to affect the catalytic performance as well. Such rare-earth metal silylamido surface species can be modified by neutral and/or monoanionic chiral ligands to afford new efficient and selective catalysts. A more general message from this study is that the structural (long-range) ordering of porous materials such as PMSs or PMOs (*p*eriodic *m*esoporous *o*rganosilicas) at the micro- and nanoscale, and in particular the pore size, is a vital criterion for assessing their suitability as supports for catalytic transformations.

Acknowledgment. We thank the Norwegian Research Council (NRC-FRINAT 171245/V30) and the University of Bergen (program Nanoscience@UiB) for generous support.

Supporting Information Available: Experimental details; microanalytical data; ^{1}H MAS NMR, ^{13}C CP/MAS NMR, and DRIFT spectra; nitrogen physisorption isotherms; SEM and TEM images; kinetic data of the catalytic IHC reactions. This material is available free of charge via the Internet at http://pubs.acs.org.

References

(1) For general references on C−N bond formation, see: (a) Beller, M.; Seayad, J.; Tillack, A.; Jiao, H. *Angew. Chem., Int. Ed.* **2004**, *43*, 3368–3398. (b) Hartwig, J. F. *Science* **2002**, *297*, 1653–1654. (c) Brunet, J. J.; Neibecker, D. In *Catalytic Heterofunctionalization*; Togni, A., Gruetzmacher, H., Eds.; Wiley-VCH: Weinheim, Germany, 2001; pp 91−141. (d) Beller, M.; Riermeier, T. H. *Transition Met. Org. Synth.* **1998**, *1*, 184–194. (e) Hegedus, L. S. *Angew. Chem., Int. Ed. Engl.* **1988**, *27*, 1113–1126.

(2) For recent reviews on catalytic hydroamination, see: (a) Müller, T. E.; Hultzsch, K. C.; Yus, M.; Foubelo, F.; Tada, M. *Chem. Rev.* **2008**, *108*, 3795–3892. (b) Hultzsch, K. C. *Adv. Synth. Catal.* **2005**, *347*, 367–391. (c) Hultzsch, K. C.; Gribkov, D. V.; Hampel, F. *J. Organomet. Chem.* **2005**, *690*, 4441–4452. (d) Hong, S.; Marks, T. J. *Acc. Chem. Res.* **2004**, *37*, 673–686. (e) Beller, M.; Tillack, A.; Seayad, J. In *Transition Metals for Organic Synthesis*, 2nd ed.; Beller, M., Bolm, C., Eds.; Wiley-VCH: Weinheim, 2004; pp 91−141. (f) Pohlki, F.; Doye, S. *Chem. Soc. Rev.* **2003**, *32*, 104–114. (g) Bytschkov, I.; Doye, S. *Eur. J. Org. Chem.* **2003**, *6*, 935–946. (h) Müller, T. E.; Beller, M. *Chem. Rev.* **1998**, *98*, 675–703.

(3) (a) Gagné, M. R.; Stern, C. L.; Marks, T. J. *J. Am. Chem. Soc.* **1992**, *114*, 275–294. (b) Gagné, M. R.; Nolan, S. P.; Marks, T. J. *Organometallics* **1990**, *9*, 1716–1718. (c) Gagné, M. R.; Marks, T. J. *J. Am. Chem. Soc.* **1989**, *111*, 4108–4109.

(4) (a) Anwander, R. In *Applied Homogeneous Catalysis with Organometallic Compounds*; Cornils, B., Herrmann, W. A., Eds.; VCH: Weinheim, Germany, 1996; Vol. 2, pp 866−892. (b) *Molecular Catalysis of Rare-Earth Elements*; Roesky, P. W., Ed.; Stucture & Bonding; 2010; p 137.

(5) For examples of rare-earth metallocene-catalyzed IHC of aminoalkenes, see: (a) Yuen, H. F.; Marks, T. J. *Organometallics* **2008**, *27*, 155–158. (b) Ryu, J.-S.; Li, G. Y.; Marks, T. J. *J. Am. Chem. Soc.* **2003**, *125*, 12584–12605. (c) Molander, G. A.; Dowdy, E. D.; Pack, S. K. *J. Org. Chem.* **2001**, *66*, 4344–4347. (d) Molander, G. A.; Dowdy, E. D. *J. Org. Chem.* **1999**, *64*, 6515–6517.

(6) For examples of rare-earth post-metallocene-catalyzed IHC of aminoalkenes, see:(a) Ge, S.; Meetsma, A.; Hessen, B. *Organometallics* **2008**, *27*, 5339–5346. (b) Rastätter, M.; Zulys, A.; Roesky, P. W. *Chem.—Eur. J.* **2007**, *13*, 3606–3616. (c) Bambirra, S.; Tsurugi, H.; van Leusen, D.; Hessen, B. *Dalton Trans.* **2006**, 1157–1161. (d) Kim, J. Y.; Livinghouse, T. *Org. Lett.* **2005**, *7*, 4391–4393. (e) Kim, Y. K.; Livinghouse, T.; Horino, Y. *J. Am. Chem. Soc.* **2003**, *125*, 9560–9561.

(7) For rare-earth metal-catalyzed asymmetric IHC of aminoalkenes, see: (a) Hannedouche, J.; Aillaud, I.; Collin, J.; Schulz, E.; Trifonov, A. *Chem. Commun.* **2008**, 3552–3554. (b) Wang, Q.; Xiang, L.; Song, H.; Zi, G. *Inorg. Chem.* **2008**, *47*, 4319–4328. (c) Yu, X.; Marks, T. J. *Organometallics* **2007**, *26*, 365–376. (d) Gribkov, D. V.; Hultzsch, K. C.; Hampel, F. *J. Am. Chem. Soc.* **2006**, *128*, 3748–3759. (e) Hong, S.; Tian, S.; Metz, M. V.; Marks, T. J. *J. Am. Chem. Soc.* **2003**, *125*, 14768–14783. (f) Vitanova, D. V.; Hampel, F.; Hultzsch, K. C. *J. Organomet. Chem.* **2007**, *692*, 4690–4701. (g) Ryu, J.-S.; Marks, T. J.; McDonald, F. E. *J. Org. Chem.* **2004**, *69*, 1038–1052. (h) O'Shaughnessy, P. N.; Knight, P. D.; Morton, C.; Gillespie, K. M.; Scott, P. *Chem. Commun.* **2003**, 1770–1771. (i) Giardello, M. A.; Conticello, V. P.; Brard, L.; Gagné, M. R.; Marks, T. J. *J. Am. Chem. Soc.* **1994**, *116*, 10241–10254.

(8) For examples of rare-earth metal-catalyzed IHC of aminoalkynes, see: (a) Reference 5a. (b) Li, Y.; Marks, T. J. *J. Am. Chem. Soc.* **1998**, *120*, 1757–1771.

(9) For examples of rare-earth metal-catalyzed IHC of aminoallenes, see: (a) Reference 5a. (b) Arredondo, V. M.; Tian, S.; McDonald, F. E.; Marks, T. J. *J. Am. Chem. Soc.* **1999**, *121*, 3633–3639.

(10) For examples of rare-earth metal-catalyzed IHC of conjugated aminodienes: (a) Yuen, H. F.; Marks, T. J. *Organometallics* **2008**, *27*, 155–158. (b) Molander, G. A.; Pack, S. K. *J. Org. Chem.* **2003**, *68*, 9214–9220. (c) Hong, S.; Kawaoka, A. M.; Marks, T. J. *J. Am. Chem. Soc.* **2003**, *125*, 15878–15892. (d) Hong, S.; Marks, T. J. *J. Am. Chem. Soc.* **2002**, *124*, 7886–7887.

(11) For examples of rare-earth metal-catalyzed IHC of aminodialkenes, aminodialkynes, and aminoalkenalkynes, see:(a) Reference 8b. (b) Li, Y.; Marks, T. J. *J. Am. Chem. Soc.* **1996**, *118*, 707–708.

(12) Zhao, J.; Marks, T. J. *Organometallics* **2006**, *25*, 4763–4772.

(13) Thomas, J. M.; Raja, R.; Lewis, D. W. *Angew. Chem., Int. Ed.* **2005**, *44*, 6456–6482, and references therein.

(14) (a) Anwander, R. *Chem. Mater.* **2001**, *13*, 4419–4438. (b) Le Roux, E.; Anwander, R. In *Modern Surface Organometallic Chemistry*; Basset, J.-M.,Psaro, R., Roberto, D., Ugo, R., Eds.; VCH Verlagsgesellschaft mbH: Weinheim, 2009; pp 455−512.

(15) (a) Copéret, C.; Chabanas, M.; Petroff Saint-Arroman, R.; Basset, J.-M. *Angew. Chem., Int. Ed.* **2003**, *42*, 156–181, and references therein.

(16) (a) Hultzsch, K. C.; Hampel, F.; Wagner, T. *Organometallics* **2004**, *23*, 2601–2612. (b) Kim, Y. K.; Livinghouse, T. *Angew. Chem., Int. Ed.* **2002**, *41*, 3645–3647. (c) Kim, Y. K.; Livinghouse, T.; Bercaw, J. E. *Tetrahedron Lett.* **2001**, *42*, 2933–2935. (d) Bürgstein, M. R.; Berberich, H.; Roesky, P. W. *Chem.—Eur. J.* **2001**, *7*, 3078–3085.

(17) For examples, see: (a) Gauvin, R. M.; Delevoye, L.; Hassan, R. A.; Keldenich, J.; Mortreux, A. *Inorg. Chem.* **2007**, *46*, 1062–1070. (b) Gauvin, R. M.; Chenal, T.; Hassan, R. A.; Addad, A.; Mortreux, A. *J. Mol. Catal. A: Chem.* **2006**, *257*, 31–40. (c) Chen, Y.; Zhu, Z.; Zhang, J.; Shen, J.; Zhou, X. *J. Organomet. Chem.* **2005**, *690*, 3783–3789. (d) Gauvin, R. M.; Mortreux, A. *Chem. Commun.* **2005**, 1146–1148. (e) Anwander, R.; Palm, C. *Stud. Surf. Sci. Catal.* **1998**, *117*, 413–420. (f) Anwander, R.; Roesky, R. *J. Chem. Soc., Dalton Trans.* **1997**, 137–138.

(18) For an example, see: Gerstberger, G.; Palm, C.; Anwander, R. *Chem.—Eur. J.* **1999**, *5*, 997–1005.

(19) D. Zhao, D.; Huo, Q.; Feng, J.; Chmelka, B. F.; Stucky, G. D. *J. Am. Chem. Soc.* **1998**, *120*, 6024–6036.

(20) The reactions have been monitored by ^{1}H NMR in sealed tubes. To avoid long reaction times, the temperature was raised up to 50 °C. Inherently, complexes **2a**/**c** afforded 90−95% conversion only after 3−6 h at 24−25 °C, where **2c** is the most active metal center.[16a,c]
(21) The influence of ionic radii on IHC has been mainly observed for lanthanides,[3a] and a reverse influence was reported for group 3 silylamido complexes employing either the same or other substrates.[6d,16a]
(22) (a) Le Roux, E.; Chabanas, M.; Baudouin, A.; de Mallmann, A.; Copéret, C.; Quadrelli, E. A.; Thivolle-Cazat, J.; Basset, J.-M.; Lukens, W.; Lesage, A.; Emsley, L.; Sunley, G. J. *J. Am. Chem. Soc.* **2004**, *126*, 13391–13399. (b) Rosier, C.; Niccolai, G. P.; Basset, J.-M. *J. Am. Chem. Soc.* **1997**, *119*, 12408–12409.
(23) (a) Kresge, C. T.; Leonowicz, M. E.; Roth, W. J.; Vartuli, J. C.; Beck, J. S. *Nature* **1992**, *359*, 710–712. (b) Beck, J. S.; Vartuli, J. C.; Roth, W. J.; Leonowicz, M. E.; Kresge, C. T.; Schmitt, K. D.; Chu, C. T. W.; Olson, D. H.; Sheppard, E. W.; McCullen, S. B.; Higgins, J. B.; Schlenker, J. L. *J. Am. Chem. Soc.* **1992**, *114*, 10834–10843.
(24) Zhang, H.; Sun, J.; Ma, D.; Weinberg, G.; Su, D. S.; Bao, X. *J. Phys. Chem. B* **2006**, *110*, 25908–25915.
(25) Solans-Monfort, X.; Filhol, J.-S.; Copéret, C.; Eisenstein, O. *New J. Chem.* **2006**, *30*, 842–850.
(26) Motta, A.; Lanza, G.; Fragalà, I. L.; Marks, T. J. *Organometallics* **2004**, *23*, 4097–4104.
(27) It is unlikely that more than 3 equiv of substrate or product molecules coordinate to the metal center, implying that a substantial amount of residual substrate and product remain in the mesopore cavities despite the washing and drying steps.

JA107963U